

Mid-infrared channel waveguides in RbPb₂Cl₅ crystal inscribed by femtosecond laser pulses.

Andrey Okhrimchuk^{a,b,*}, Vladimir Mezentsev^c, and Ninel Lichkova^d

^a D.Mendeleev University of Chemical Technology of Russia, Miusskaya Sq. 9, Moscow 125047, Russian Federation.

^b Fibre Optics Research Centre of RAS, 38 Vavilov Street, Moscow 119333, Russian Federation.

^c Aston University, Aston Triangle, Birmingham B4 7ET, UK

^d Institute of Microelectronics Technology of RAS, Chernogolovka 142432, Russian Federation

* Corresponding author, E-mail: a.okhrim@yandex.ru

Keywords:

Femtosecond inscription;

Cladding waveguide;

Leaking waveguide mode;

Abstract

Tubular cladding waveguide was inscribed in crystal volume by a femtosecond laser operating at 0.8 μm . The waveguide sustains a single leaking mode at wavelength of 3.39 μm . Propagation losses were investigated experimentally and theoretically at wavelengths of 1.58 μm and 3.39 μm . Measured losses were found to be as low as 1.4 dB/cm at 1.58 μm and 5.1 dB/cm at 3.39 μm . Complex propagation constants for leaking modes were obtained by numerical mode analysis. It was found, that mode leakage is a major factor of losses at wavelength of 3.39 μm .

1. Introduction

The RbPb₂Cl₅ (RPC) crystal is very attractive for mid infrared (Mid-IR) applications as a laser host material because energy of the most energetic phonon is extremely low in this crystal (203 cm^{-1} , [1]). Moreover it is moisture resistant in contrary to most of chloride crystals and has a wide transparency window ranging from 0.3 μm to 20 μm covering the whole VIS and Mid-IR. As a result of these outstanding properties Mid-IR oscillation was demonstrated in RPC:Pr³⁺ and RPC:Dy³⁺ crystals at room temperature [2,3]. However efficient pumping of a conventional laser element by a laser beam propagating in free space is problematic because of low segregation coefficient of rare-earth ions in this crystal. Waveguide architecture of a laser allows keeping high pump intensity on the longer optical path in comparison with the free space scheme. Thus we suggest that a waveguide laser based on the rare earth doped RbPb₂Cl₅ crystal should have higher efficiency and lower threshold than a bulk laser. Feasibility of the waveguiding approach is demonstrated in fs-written channel waveguides in YAG:Yb³⁺ crystal [4], YVO₄:Nd crystal [5], ZBLAN:Tm³⁺ glass [6], YAG:Tm [7], ZnSe:Cr²⁺ [8,9], ZnSe:Fe²⁺ [9,10] crystals. In these works stress-

induced waveguides and depressed cladding waveguide architecture were used [12,13]. Tubular cladding (*or depressed cladding*) architecture of a waveguide allows to keep waveguide core unmodified and to avoid large mechanical stress, thus spectroscopic properties and optical homogeneity of laser medium do not degrade after inscription [5-11]. This results in low propagation loss and high laser efficiency. Applicability of this approach for mid-IR laser was demonstrated on the example of the waveguides inscribed in ZnSe crystal doped with Cr²⁺ and Fe²⁺ ions [8-10]. However ZnSe crystal has spectroscopic restriction for effective operation at room temperature at wavelengths higher 4 μm because of multi-phonon quenching in the *d*-element active ions due to high electron phonon coupling. Unfortunately *f*-elements that have basically lower electron-phonon coupling are very poor soluble in ZnSe crystal. The lattice of RPC crystal far better segregates *f*-elements, thus it is attractive to implement waveguide architecture to this laser host.

The femtosecond writing causes negative refractive index change in RPC:Dy crystal [14], The obtained maximal magnitude of the index change is about 10 times lower than in ZnSe crystal as followed from numerical aperture of 0.37 for the tubular waveguide [9]. Low value of refractive index change in RPC crystal raises the question of applicability of tubular architecture to this crystal, because cladding thickness is comparable with the wavelength in mid-IR, and the mode leakage could degrade performance of the waveguide laser. In this paper we report first results on inscription and characterization of a channel waveguide in RPC crystal and show that the mode leakage is a main factor that should be taken into account when writing depressed cladding waveguide in RPC crystal for mid-IR applications.

2. Crystal growth and sample preparation for inscription.

The single crystal of RPC:Dy double salt was grown by the vertical Bridgman method in the two-zone furnace in a silica tube crucible with diameter of 7 mm. Crystal growth was started in random crystallization direction, so orientations of investigated samples were arbitrary. Details of crystal growth can be found in [15]. Concentration of Dy³⁺ ions in the crystal was determined by ICP-MS method and was found to be as high as $2.8 \times 10^{-19} \text{ cm}^{-3}$.

A rectangular plate of the crystal with thickness of 4 mm was cut from the central part of cylindrical bowl of the crystal so that crystal growth direction was parallel to the large plate facets. These facets had sizes of $23 \times 6 \text{ mm}^2$ and were polished with the laser grade.

3. Femtosecond laser inscription setup

Femtosecond laser beam used for inscription was generated by a Ti:Sapphire laser system with a regenerative amplifier operating at wavelength of 0.8 μm . Repetition rate was 1 kHz, and FWHM pulse duration was 110 fs. M^2 parameter of the beam did not exceed 1.05. A motorized polarization attenuator was used to control energy of the laser pulse entering the sample. The sample was mounted on Aerotech high precision three-dimensional translation stage. The laser beam was focused in the crystal under its surface at different depth from the range of 50 – 200 μm by the 100x Mitutoyo lens with NA=0.55. A cylindrical defocusing lens with focal distance of 340 mm was placed before the Mitutoyo lens. The cylindrical lens ensured astigmatic

focusing hence preventing the beam from destructive influence of Kerr self-focusing [16]. Suppression of self-focusing is an especially important for inscription of smooth tracks in RPC crystal, as it has high non-linear refractive index n_2 , which is by factor of 21 larger than that in fused silica [14]. Installation of the cylindrical lens followed by the strong focusing lens leads to the two orthogonal beam waists, the inscription process happens in the waist nearest to Mitutoyo lens due to highest intensity there. Calculated diffraction diameters of this waist were 1.1 μm and 14 μm , and the biggest diameter was aligned along an inscribed track. It was shown that the elliptical beam waist allows inscribing perfect smooth tracks and low loss tubular cladding waveguides in YAG crystal [11,16]. Examples of tracks written in RPC crystal with and without the cylindrical lens are shown in Fig.1.

4. Waveguide architecture and fabrication.

Since the refractive index change is negative in RPC crystal [14], waveguides with depressed cladding composed by closely spacing parallel tracks were written in the crystal [5-12]. The pulse energy and the scanning speed were chosen to satisfy two fairly contradictory requirements for each elementary track, that is high enough refractive index change (should exceed 10^{-3}) and visible smoothness of a track (checked by microscopic inspection). The scanning speed was set to 0.5 mm/s, and polarization of writing beam was along scanning direction. Five waveguides differed in shape and in size of the core were written parallel to each other along the entire length of the rib plate of 23 mm under slightly different pulse energies shown in Table 1, and they are about 4 times exceeding energy at the inscription threshold, that is 0.2 μJ [14]. Each waveguide consisted of 24 tracks with lowered refractive index. A ring of the inscribed tracks forms a tubular cladding surrounding an unmodified core of the waveguide. End view of a waveguide with a nearly circular core is presented in Fig.1. Other waveguides are differed by core diameters (W and H in Fig.1) and by an interval between tracks. Geometrical and inscription parameters are summarized in Table 1.

In order to eliminate mechanical stress around tracks the crystal with inscribed waveguides was thermally treated at 230°C during 70 hours in evacuated and sealed quartz ampoule. Then the sample was cut perpendicular to direction of waveguides in two equal parts with lengths of 11 mm, and then ends of both crystals were polished in a single block with the laser grade. Below in the text we will refer to these crystal parts as *the crystal #1* and *the crystal #2*.

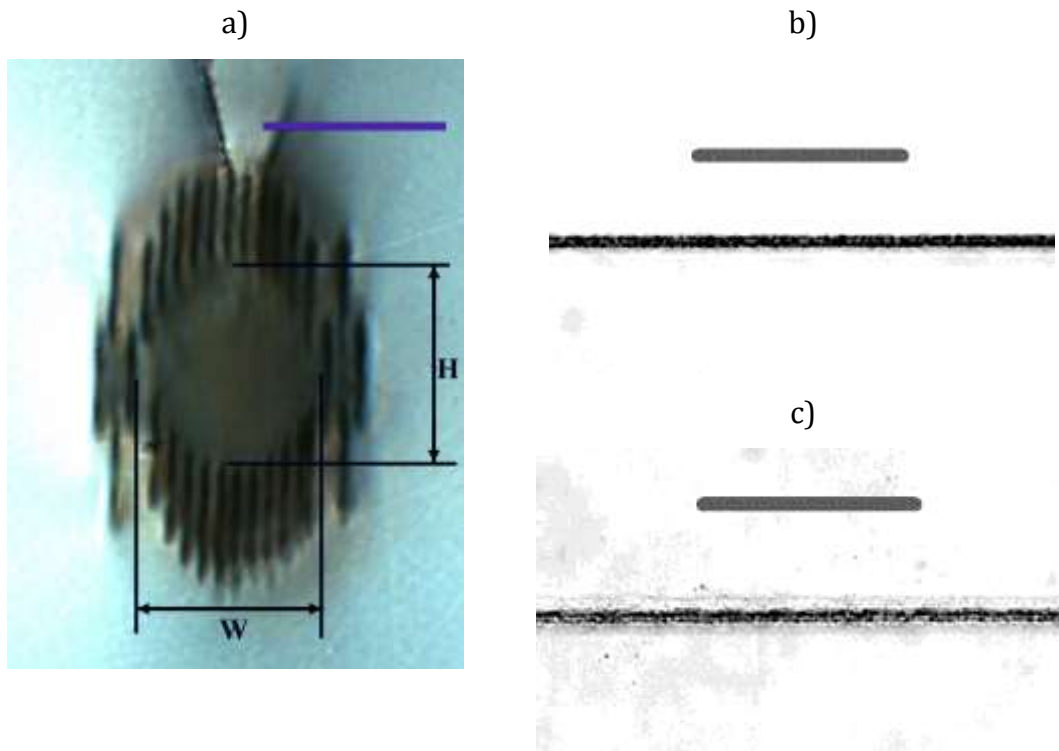


Fig. 1. a) Microscopic end view of the waveguide # 5 with a circular core. The scale bar corresponds to 40 μm . b) Top view of tracks written by focusing b) with microscopic lens of $\text{NA}=0.55$ and cylindrical defocusing lens with focal distance of 340 mm under pulse energy of 0.57 μJ and scanning speed of 1 mm/s, and c) with microscopic lens of $\text{NA}=0.5$ and without a cylindrical lens under pulse energy 0.48 μJ and scanning speed of 0.5 mm/s. The scale bars are 50 μm for b) and c).

5. Waveguide characterization

Mode structure and waveguides losses were investigated with single mode Er-fiber laser operating at 1.58 μm and nearly single mode He-Ne gas laser operating at 3.39 μm . We used a two lens focusing system to optimize coupling of the laser beam with the input end of a waveguide in order to excite predominantly the fundamental mode. At 1.58 μm an image of intensity distribution at waveguide output was formed by a microscopic lens with focal distance of 19 mm on Spiricon SP-1550M phosphorus coated CCD camera. At the wavelength of 3.39 μm the image was formed by BaF_2 lens with focal distance of 25 mm on Spiricon Pirocam-III piroelectric camera. The waveguides demonstrated a single mode behavior at both 1.58 μm and 3.39 μm (Fig.2). The mode radii measured at $1/e^2$ intensity level are summarized in Table 1.

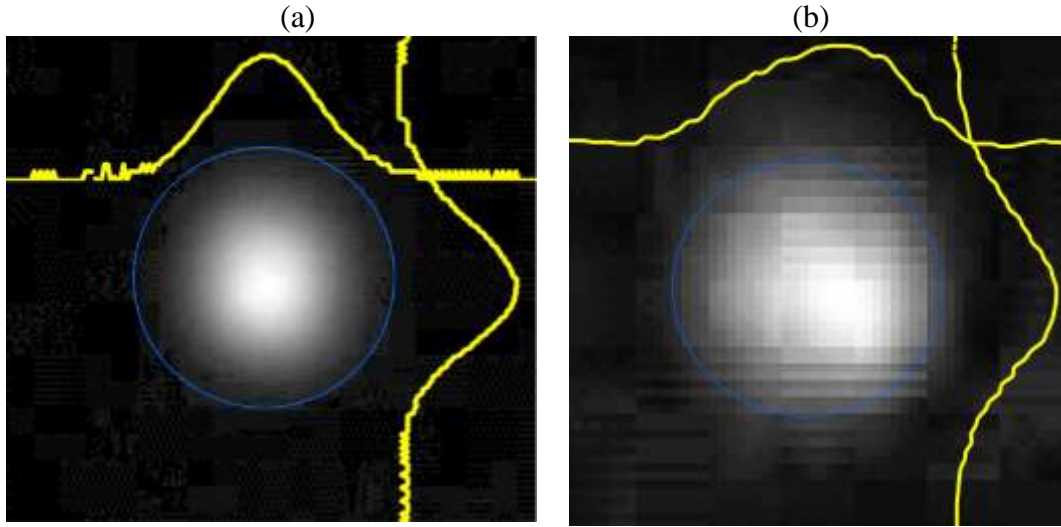


Fig. 2. Measured mode intensity 2D distribution (grey) and its profiles (yellow lines) at the output of the waveguide #5 of the crystal #1 at wavelength of 1.58 μm (a) and 3.39 μm (b). Boundary of the circular core of 40 μm diameter is shown by the blue thin line.

Table.1. Measured losses and radii of fundamental modes (x is for horizontal profile, and y is for vertical profile).

Waveguide#	E_{in} (μJ)	W (μm)	H (μm)	Mode radii				Losses (dB/cm)	
				$\lambda=1.58 \mu\text{m}$		$\lambda=3.39 \mu\text{m}$		$\lambda=1.58 \mu\text{m}$	$\lambda=3.39 \mu\text{m}$
				ω_x (μm)	ω_y (μm)	ω_x (μm)	ω_y (μm)		
1	0.93	37	37	20.8	21.7	26.1	29	8.1 ± 0.4	9.8 ± 0.4
2	0.93	37	35	20.4	20.6	23.1	34	2.4 ± 0.4	4.8 ± 0.4
3	0.93	41	36	18.2	19.3	23.4	27	1.6 ± 0.4	7.9 ± 0.4
4	0.93	56	39	22.2	21.3	19.4	22.5	3.9 ± 0.4	4.8 ± 0.4
5	0.77	40	40	17.9	22.0	24.9	27.5	1.4 ± 0.4	5.1 ± 0.4

In order to measure propagation losses we have adapted to waveguides investigated the “cut-back” method that is famous in fiber optics. The measurements were done in two stages. At the first stage the crystal #1 (see previous chapter), was put on a high quality polished glass substrate by its closest to waveguides facet. After laser beam have being coupled to a waveguide in crystal #1, the crystal #2 was put on the same substrate in the same manner and attached to the crystal #1 output end by end providing butt coupling. Distance between waveguides and closest facet was identical in both crystals (around 120 μm), so waveguides ends had automatically the same vertical coordinate. Horizontal position of the crystal #2 was tuned by gliding translation on the substrate and along the output end of the crystal #1, while a mode image and intensity at the output end of crystal #2 was monitored on a camera. We strived for a maximum output from a waveguide in the crystal #2 by tuning its

position relative to the crystal #1. In such arrangement the corresponding waveguides are aligned to straight lines where they were before the cut. Output power from a waveguide in the crystal #2 P_2 was measured, and then the crystal #2 was removed. Finally output power from a waveguide remaining in the crystal #1 P_1 was measured. Loss was calculated according a formula:

$$L = 10 \log \left(\frac{P_2}{P_1} \right) / d \quad (1),$$

where d is the waveguide length for crystal #2. Lowest loss was obtained for a waveguide with the lowest ellipticity in cross section (#5). Data for measured losses are summarized in Table 1.

6. Theoretical investigations and discussions

Since lowest propagation loss was measured for the waveguide #5, we have made calculations of the mode composition and the leakage loss for this waveguide. The numerical analysis has been performed with Comsol Multiphysics code (ver. 3.5). The full vectorial Maxwell mode solver was exploited for solving 2D eigenvalue problem to find the propagation constant (the effective mode refractive index). Geometry used in calculations is shown in Fig.3. Cross section of an elementary track was modeled by an ellipse of $22 \times 2 \mu\text{m}^2$ that is nearly equivalent to real a track in the waveguide No.5. (Fig.1). The refractive index change was assumed to be constant within a track. Small homogeneous refractive index increase in the core Δn_{core} due to compressive stress arising from the cladding was included in the analysis.

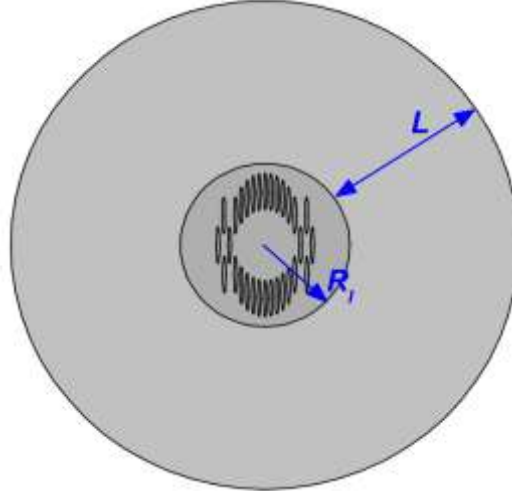


Fig.3. Geometry of numerical mode analysis. $R_i=50 \mu\text{m}$, $L=100 \mu\text{m}$.

Investigated waveguides are characterized by significant leakage loss in mid-IR, because effective thickness of the depressed cladding is comparable with the wavelength. Perfectly matched layer (PML) at the boundary was used to simulate propagation of leaking radiation in the infinite medium. We have used a quadratic dependence of absorption in the PML on the distance to the center. The complex refractive index in PML region satisfies the formula [17]:

$$n_{PML} = n_0 - ik_m \left(\frac{r - R_i}{L} \right)^2 \quad (2),$$

where n_0 is the refractive index of RPC crystal ($n_0=2.12$ [3]), r is the distance to the center, R_i is the inner radius of PML, and L is the thickness of PML (Fig.3), k_m is maximum of imaginary part of refractive index, realized on PML outer boundary.

Numerical mode analysis was performed in two stages and included finding of refractive index change. Firstly we optimized the PML in assumption of refractive index change in the cladding tracks $\Delta n = -1.5 \times 10^{-3}$ that was obtained for a track written in close experimental condition [14], and for refractive index change in the core $\Delta n_{core} = 0$. On the second stage the refractive index changes were made specific.

On the first stage solutions for wavelength of $3.39 \mu\text{m}$ with different absorption coefficient in the PML from the range $0.0001 - 0.04$ were analyzed for defining the PML that ensures minimum impact of reflection from PML outer boundary. We found that the optimum PML is realized with the absorption parameter $k_m = 0.002$ based on the following consideration. Three representative solutions for the intensity distribution are shown in Fig.4 for different values of absorption in the PML. The reflection from outer boundary is clearly seen at low absorption, and the PML itself obviously reflects radiation at high absorption. Mostly diffusive distribution of radiation intensity out of the cladding is observed at $k_m = 0.002$, indicating that this is optimum value most adequately describing the mode leakage.

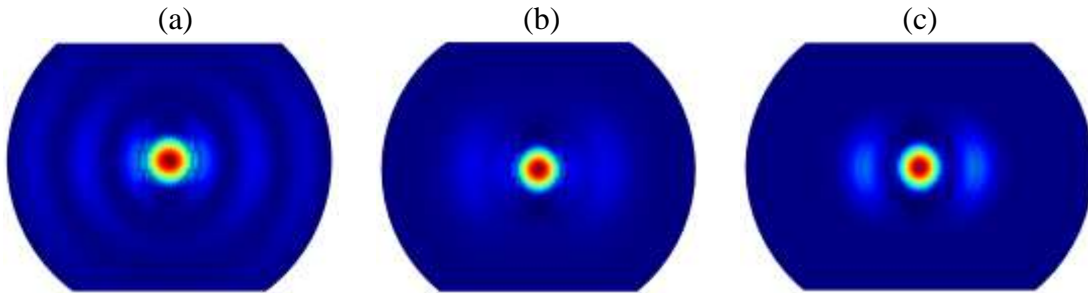


Fig.4. Solution of the eigenvalue problem for three representative PML absorption values: a) $k_m = 0.0001$; b) $k_m = 0.002$; c) $k_m = 0.02$. Thin dark lines denote boundaries of the tracks and PML.

The dependence of effective refractive index on the absorption in PML is presented in Fig.5. It is interesting that there are flat extremes for real and imaginary parts of the refractive at the PML absorption $k_m = 0.002$. The decrease of the real part and increase of the imaginary part with increase of PML absorption relative to the optimum corresponds to the increase of PML contribution to wave guiding and attenuation of the fundamental mode due to PML. There are sharp extremes at lower absorption region corresponding to mode rebuilding due to the increased impact of the outer boundary.

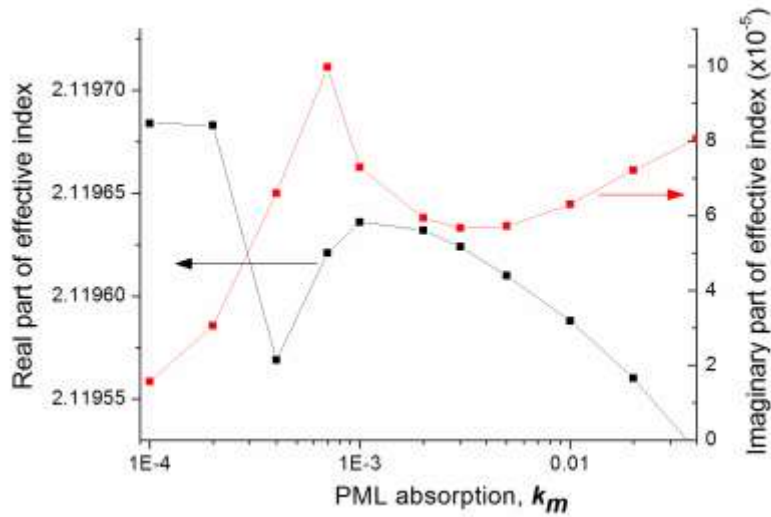


Fig.5. Theoretical dependences of the effective mode index components upon absorption in PML for the fundamental mode at the wavelength of 3.39 μm . Refractive index change in a track $\Delta n = -1.5 \times 10^{-3}$, in the core $\Delta n_{\text{core}} = 0$.

On the second calculation stage refractive index change in an elementary track and in the core was fitted. We fixed $k_m = 0.002$ and varied the refractive index changes Δn and Δn_{core} while iteratively solving eigen value problem for 1.58 μm and 3.39 μm , and comparing calculated mode sizes with those measured in the experiment (ω_x and ω_y). Best fitting was found for refractive index change in a track $\Delta n = -10^{-3}$, and small increase of refractive index in the core $\Delta n_{\text{core}} = 1.5 \times 10^{-4}$. Calculated and measured mode radii are compared in Table 2.

Table 2. Calculated and measured mode parameters for the waveguide #5.

		LP ₀₁ mode radii at 1.58 μm		LP ₀₁ mode radii at 3.39 μm		Losses (dB/cm)	
		ω_x	ω_y	ω_x	ω_y	at 1.58 μm	at 3.39 μm
		(μm)	(μm)	(μm)	(μm)		
Experiment		17.9	22.0	24.9	27.5	1.4±0.4	5.1±0.4
Theory	LP ₀₁	18.7	20.6	21.2	25.5	8.7*10 ⁻³	5.8
	LP ₁₁	-	-	-	-	0.73	-

At 3.39 μm the modeled waveguide was found to maintain two fundamental LP₀₁ modes with identical intensity distribution and degenerated by polarization. At 1.58 μm in addition to the fundamental modes two lower LP₁₁ modes degenerated on polarization were found. Effective propagation indexes of degenerate modes were found to be equal to each other at both wavelengths.

Calculated imaginary parts of the mode effective refractive indexes were found to be as low as 2.5×10^{-8} and 2.1×10^{-6} for LP₀₁ and LP₁₁ modes correspondingly at 1.58 μm and 3.6×10^{-5} at 3.39 μm wavelength. This results in leakage loss of 8.7×10^{-3} dB/cm for LP₀₁ and 0.73 dB/cm for LP₁₁ at wavelength of 1.58 μm , and 5.8 dB/cm at 3.39 μm (for LP₀₁). The parameters are summarized in Table 2.

Fairly good matching of the calculated and measured losses at 3.39 μm wavelength allows us to conclude that the mode leakage is a dominant mechanism of loss for the waveguide #5, which demonstrates the best performance. Such sufficiently high loss will obviously prevent efficient lasing in mid-IR. Leakage loss could be reduced through increase of the refractive index change in the cladding, like in the case of ZnSe crystal. However larger change of refractive index through rise of pulse energy is restricted [14]. Unexploited possibility in this connection is optimization of the polarization orientation relative crystallographic axes, as RPC crystal belongs to the monoclinic class, and it is expected that it possesses strong anisotropy. The basis for this view is the strong dependence of the waveguide propagation loss on the direction of writing beam polarization in the orthorhombic YAP crystal [18].

On the other hand one can notice while inspecting Fig.4 that the mode leakage mainly goes through left and right sides of the waveguides cladding. In this concern we hope that the considered waveguide architecture could be improved by adding some tracks to the cladding sides, and this way leakage will be reduced to acceptable value. Another way is to increase diameter of the core, but this move could lead to multimode operation. We assume in this connection that the solution to the problem may lie in the rejection of simple depressed cladding architecture having a Gaussian fundamental mode and formation of the specially structured core that supports single mode behavior even with core of large diameter [13].

Contrary to 3.39 μm , at wavelength of 1.58 μm the calculated losses is more than 100 times lower than measured one, which presumably thought to be for fundamental mode. Obviously that the scattering on track imperfections makes great contribution to propagation loss for LP₁₀ mode in short wavelength region, and besides couples LP₀₁ and LP₁₁ modes, that also increase losses for LP₀₁ mode [14]. Although losses for short wavelengths could raise problems for efficient pumping, they should not degrade laser cavity in Mid-IR.

7. Conclusions

A single mode depressed cladding waveguide is inscribed by femtosecond pulses in RbPb₂Cl₅ crystal for the first time to the best of our knowledge. Guidance of light up to wavelength of 3.39 μm is demonstrated. The circular core waveguide possesses lowest loss that was as low as 5.1 dB/cm at wavelength of 3.39 μm . Propagation loss is mainly due to mode leakage at this wavelength. Evidence of loss of other nature was found for 1.58 μm , and the total loss was measured to be 1.4 dB/cm at this wavelength. Distinguishing feature of femtosecond writing in RbPb₂Cl₅ crystals is very high self-focusing, which prevents smoothed writing by ordinary beam of circular cross-section profile, but astigmatic focusing is shown to be a solution to overcome this difficulty.

Acknowledgment

This work was supported by The Ministry of Education and Science of Russian Federation, grant #14.Z50.31.0009, and Leverhulme Trust funding VP1-2011-025 (UK).

References

- [1] K. Rademaker, W. F. Krupke, R. H. Page, and S. A. Payne, "Optical properties of Nd³⁺- and Tb³⁺-doped KPb₂Br₅ and RbPb₂Br₅ with low nonradiative decay," *J. Opt. Soc. Am. B* **21**, 2117–2129 (2004).
- [2] A.G. Okhrimchuk, L.N. Butvina, E.M. Dianov, N.V. Lichkova, V.N. Zagorodnev, A.V. Shestakov, "New laser transition in the RbPb₂Cl₅:Pr³⁺ crystal in the 2.3 – 2.5 μm wavelength range", *Quantum Electronics*, **36**, No.1, P41-44 (2006).
- [3] A.G. Okhrimchuk, L.N. Butvina, E.M. Dianov, I.A. Shestakova, N.V. Lichkova, V.N. Zagorodnev, and A.V. Shestakov, "Optical spectroscopy of the RbPb₂Cl₅:Dy³⁺ laser crystal and oscillation at 5.5 μm at room temperature", *Journal of Optical Society of America B*, **24**, 2690-2695 (2007).
- [4] J. Siebenmorgen, T. Calmano, K. Petermann, and G. Huber, "Highly efficient Yb:YAG channel waveguide laser written with a femtosecond-laser", *Optics Express*, **18**, 16035-16041 (2010).
- [5] Y. Jia, F. Chan, and J.R.V. Aldana, "Efficient continuous-wave laser operation at 1064 nm in Nd:YVO₄ cladding waveguides produced by femtosecond laser inscription", *Optics Express*, **20**, 16081-16806 (2012).
- [6] D.G. Lancaster, S. Gross, H. Ebendorff-Haidepriem, K. Kuan, T.M. Monro, M. Ams, A. Fuerbach, and M.J. Withford, "Fifty percent internal slope efficiency femtosecond direct-written Tm³⁺:ZBLAN waveguide laser", *Optics Letters*, **36**, 1587-1589 (2011).
- [7] Y. Ren, G. Brown, A. Ródenas, S. Beecher, F. Chen, and A.K. Kar, "Mid-infrared waveguide lasers in rare-earth-doped YAG," *Opt. Lett.* **37**, 3339-3341 (2012).
- [8] J.R. Macdonald, S.J. Beecher, P.A. Berry, G. Brown, K.L. Schepler, and A.K. Kar, "Efficient mid-infrared Cr:ZnSe channel waveguide laser operating at 2486 nm", *Optics Letters*, **38**, 2194-2196 (2013).
- [9] S. A. McDaniel, A. Lancaster, J. W. Evans, A. K. Kar, and G. Cook, "Power scaling of ultrafast laser inscribed waveguide lasers in chromium and iron doped zinc selenide," *Opt. Express*, **24**, No.4, P. 3502 (2016).
- [10] A. Lancaster, G. Cook, S. A. McDaniel, J. Evans, P. A. Berry, J. D. Shephard, and A. K. Kar, "Mid-infrared laser emission from Fe:ZnSe cladding waveguides," *Appl. Phys. Lett.*, **107**, No.3, P.031108(2015).
- [11] A.G. Okhrimchuk, V.K. Mezentsev, A.V. Shestakov, and I. Bennion, "Low loss depressed cladding waveguide inscribed in YAG:Nd single crystal by femtosecond laser pulses", *Optics Express*, **20**, 3834 (2012).
- [12] A. Okhrimchuk, "Femtosecond Fabrication of Waveguides in Ion-Doped Laser Crystals," in *Coherence and Ultrashort Pulse Laser Emission*, F. J. Duarte, Ed. InTech, 2010.
- [13] Y. Jia, C. Cheng, J. R. Vázquez de Aldana, G. R. Castillo, B. del R. Rabes, Y. Tan, D. Jaque, and F. Chen, "Monolithic crystalline cladding microstructures for efficient light guiding and beam manipulation in passive and active regimes" *Sci. Rep.*, **4**, 5988 (2014).
- [14] A.G. Okhrimchuk, V.K. Mezentsev, N.V. Lichkova, V.N. Zagorodnev, "Femtosecond writing in monoclinic RbPb₂Cl₅:Dy³⁺ crystal", *Optical Materials*, **43**, 1-5 (2015).
- [15] N.V. Lichkova, V. N. Zagorodnev, L.N. Butvina, A.G. Okhrimchuk, and A. V. Shestakov, "Preparation and optical properties of rare-earth-activated alkali metal lead chloride crystals," *Inorganic Materials*, **42**, 81–88 (2006).
- [16] A.G. Okhrimchuk, V. K. Mezentsev, H. Schmitz, M. Dubov and I. Bennion, "Cascaded nonlinear absorption of femtosecond laser pulses in dielectrics", *Laser Physics*, **19**, No. 7, 1415-1422, (2009).
- [17] H. Karakuzu, M. Dubov and S. Boscolo, "Control of the properties of micro-structured waveguides in lithium niobate crystal", *Optics Express*, **21**, 17122-17130 (2013).
- [18] W. Nie, R. He, C. Cheng, U. Rocha, J. Rodríguez Vázquez de Aldana, D. Jaque, and F. Chen, "Optical lattice-like cladding waveguides by direct laser writing: fabrication, luminescence, and lasing," *Opt. Lett.*, **41**, 2169–72 (2016).